

## Sensor and Simulation Notes

Note 456

May 2001

### **Automated Time Domain Antenna Range Initial Implementation**

W. Scott Bigelow, Everett G. Farr, and Leland H. Bowen  
*Farr Research, Inc.*

Tyrone C. Tran, Carl E. Baum, and William D. Prather  
*Air Force Research Laboratory, Directed Energy Directorate*

### **Abstract**

For organizations engaged in the development of antenna designs, conventional frequency domain antenna measurement systems represent a huge initial cost, and a significant barrier to entry into the field. When characterizing ultra-wideband antennas, the cost of frequency domain measurements is even greater, because data must be taken at many frequencies, requiring additional time. A time domain antenna range addresses these cost and time issues. Such ranges will have one-quarter the cost of a frequency domain range, and will provide meaningful data over two decades of bandwidth in a single measurement, in either frequency or time domain. They will also be readily stowed and deployed.

Here, we describe development of a prototype time domain antenna range, which provides fully automated scanning of antenna orientations (azimuth and elevation). At each orientation, control software commands a digital sampling oscilloscope to acquire a measurement and return the resulting data to a computer for display, storage, and processing. Processing of acquired data to determine antenna gain can be done online in near-real-time.

## **1. Introduction**

For organizations engaged in the development of new antenna designs, antenna measurement systems represent a huge initial cost, and a significant barrier to entry into the field. Antenna measurement systems typically use a frequency domain vector network analyzer (VNA) and anechoic chamber or large outdoor range. The total cost of such systems exceeds \$300,000. When ultra-wideband (UWB) antennas must be characterized, the cost of frequency domain measurements is even greater, because the data must be taken at many frequencies, requiring additional time.

To address these cost and time issues, technology is now available that permits the characteristics of antennas to be measured directly in the time domain. Such time domain antenna ranges will have one-quarter the cost of a conventional frequency domain range. Moreover, they will provide meaningful measurements over two decades of bandwidth, in either the frequency or time domain. They will also be readily stowed and deployed, as required.

This note documents our successful efforts to develop a prototype automated time domain antenna range. This prototype features the hardware and software necessary to achieve computer control over all basic operations. The software provides fully automated scanning of antenna orientations (azimuth and elevation) for any user-specified test protocol. At each orientation, the software commands a digital sampling oscilloscope (DSO) to acquire a measurement and return the resulting waveform data to the controlling computer for display, storage, and processing. Online processing of acquired boresight data, including determination and display of the effective antenna gain, can be done in near-real-time. The current implementation is scalable to provide automated characterization of antennas for all orientations.

In the next sections, we compare conventional frequency domain ranges and the new time domain range approach, highlighting the advantages of the latter. In subsequent sections, we summarize the accomplishments leading to the current prototype automated range. We conclude by indicating the planned direction of future efforts.

## 1.1 Frequency Domain Range Description

Most currently available antenna ranges are operated in the frequency domain, using swept continuous wave (CW) techniques. The basic components of such a range are a VNA, a transmit antenna (a sensor if used in receive mode), an azimuth–elevation (AZ–EL) positioner, and the antenna under test (AUT). Figure 1 depicts such a configuration, augmented by a computer controller. One must operate such a range either within the quiet zone of an anechoic chamber, or outdoors, with both antennas located far above the ground and far from any other reflective objects. Frequency domain data obtained on such a range is sometimes converted to the time domain to gate out residual reflections, and then returned to the frequency domain.

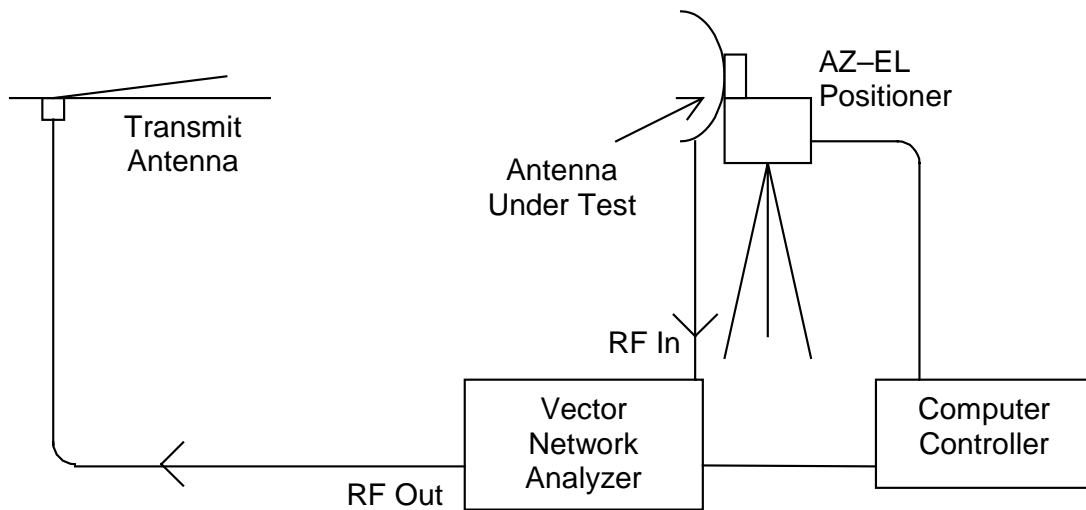


Figure 1. Frequency domain antenna measurement system.

## 1.2 Time Domain Range Description

One could build a time domain antenna range from parts similar to those of a frequency domain range merely by replacing the VNA with a pulser and an oscilloscope. Figure 2 depicts a typical system. Note that such a system does not require an anechoic chamber, because reflections from the walls or ground can be time-gated out. Note also that a pulser and oscilloscope cost much less than the VNA they replace. We provide cost comparisons for the electronic components of both systems later.

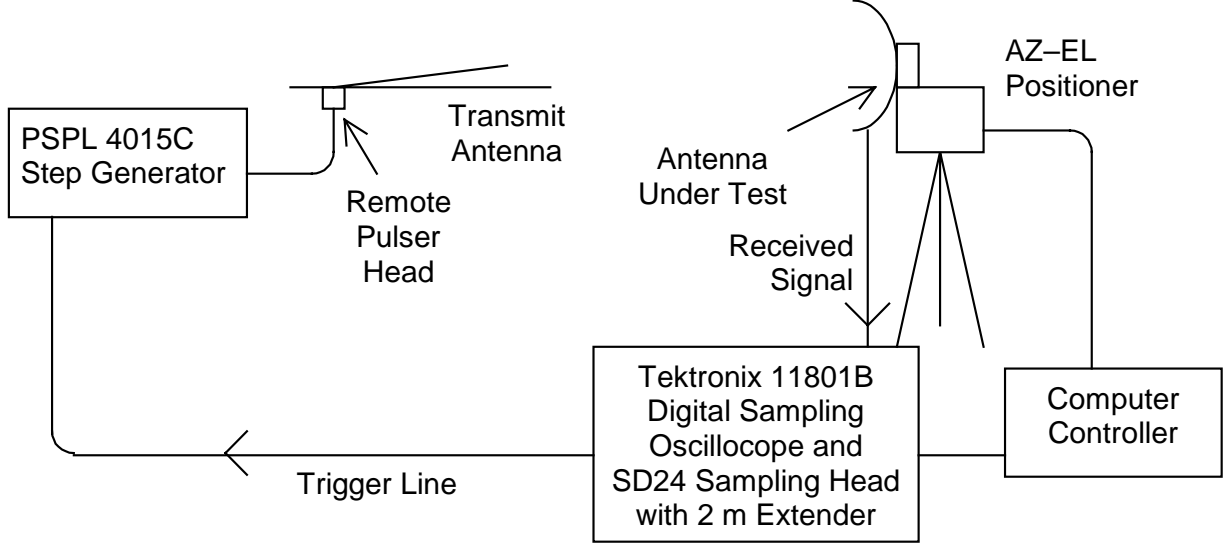


Figure 2. Time domain antenna measurement system.

### 1.3 Confirmation of the Validity of the Time Domain Method

We summarize available data confirming the equivalence of the standard frequency domain antenna measurement method and the time domain method described here. To do so, we briefly summarize the method of converting impulse response to gain, and we provide comparisons to frequency domain data taken at a standard frequency domain range.

The method of measuring the normalized impulse response of an antenna has been described in detail in many references, but perhaps most succinctly in [1]. Using the configuration of Figure 2, we record a raw antenna response at the sampling head of the oscilloscope. We obtain the impulse response of the antenna by measuring the pulser waveform into  $50 \Omega$ , measuring the impulse response of the transmit antenna, and deconvolving these and all other system responses from the raw antenna data. From this we obtain the normalized impulse response,  $h_N(t)$ , of the antenna. An example of  $h_N(t)$  for an IRA with an 18-inch diameter is shown in Figure 3, in both the time and frequency domains. These data were originally reported in [2]. To convert this impulse response to effective gain, we use the formula

$$G(\omega) = \frac{4\pi}{\lambda^2} |h_N(\omega)|^2 = \frac{4\pi f^2}{c^2} |h_N(\omega)|^2 \quad (1)$$

where  $h_N(\omega)$  is the Fourier transform of the normalized impulse response as a function of frequency, and  $c$  is the speed of light in vacuum.

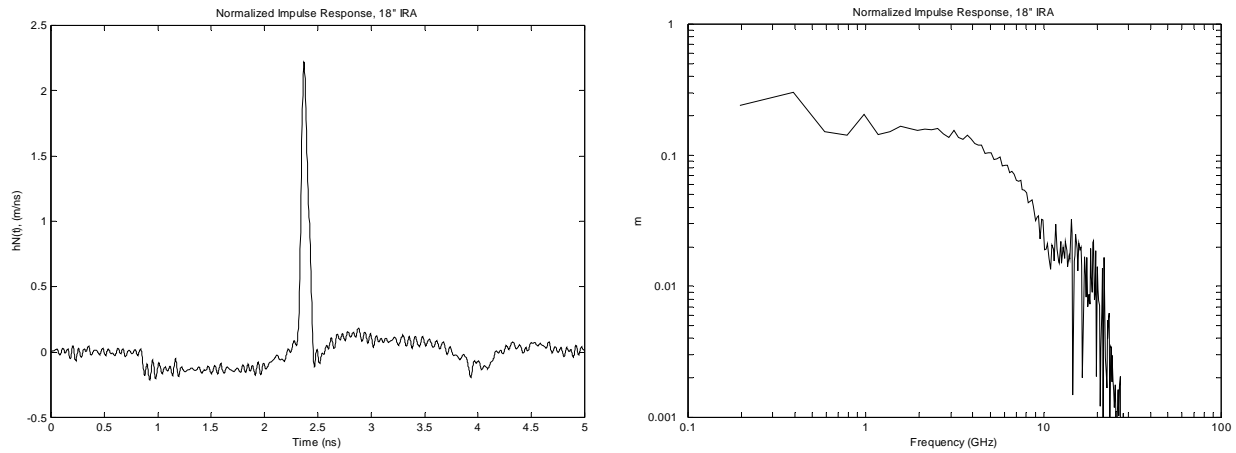


Figure 3. Normalized impulse response of an 18-inch diameter IRA in the time domain (left) and in the frequency domain (right).

The co-polarized boresight gain for the 18-inch IRA is shown in Figure 4 for both time domain (Farr Research, Inc.) and frequency domain (Mission Research Corp.) measurements. The data are an extremely close match. This result confirms the validity of the time domain antenna measurement methodology.

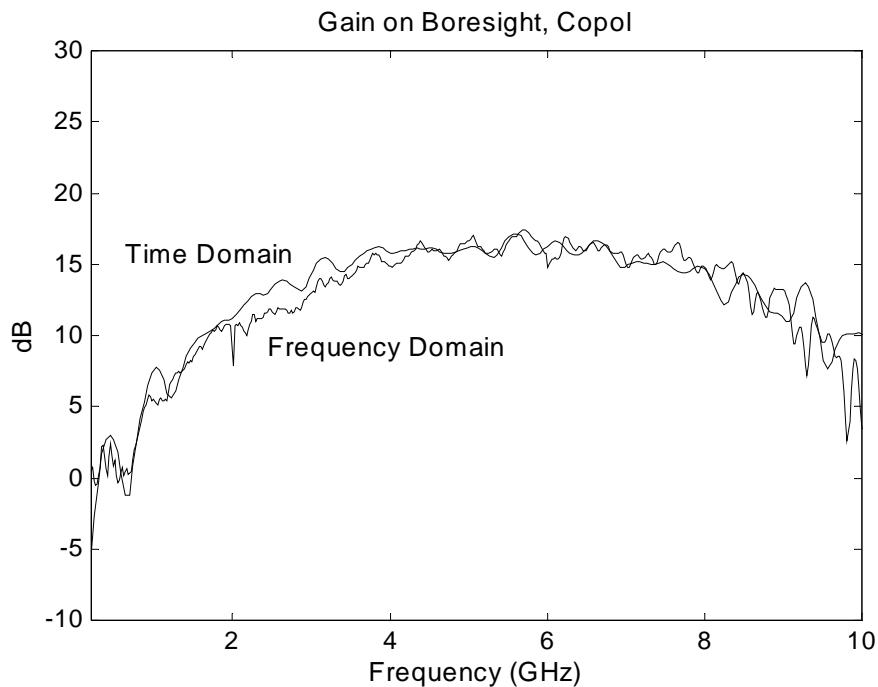


Figure 4. Comparison of the gain of the 18-inch diameter IRA on boresight, as derived from time domain and frequency domain data.

## **1.4 Relative Advantages of Working in the Time Domain**

We highlight three distinct advantages of antenna ranges operating in the time domain. These include lower cost, relaxed requirements for temperature stability, and convenience and deployability.

### **1.4.1. Lower Cost**

We first consider the cost advantages of time domain antenna ranges over frequency domain ranges. The two areas where the ranges have significantly different costs are in the electronics, and in the physical layout of the range.

The VNA is, by far, the most expensive electronic component of a frequency domain range. VNAs are available in two varieties, integrated systems, and systems assembled from components. An integrated VNA, such as the Agilent Technologies Model 8720, at about \$70,000, is far more economical than a VNA assembled from components, such as the Model 8510, at \$170,000 or more.

For antenna pattern measurements in the frequency domain, there is a clear advantage in using the more expensive VNA assembled from components. A long cable has to run from the VNA to the transmitter, as shown in Figure 1. This cable has to be a little longer than the antenna separation, which is typically 10 to 20 meters. Since there is significant high-frequency loss in such a long cable, one would prefer to run intermediate frequency (IF) signals out to the transmitter on the long cable, and then mix up to the desired frequency just before radiating the signal. This approach leads to improved precision and dynamic range, but it requires a VNA assembled from components.

The electronics associated with a time domain system cost much less. Our system employs a 4-volt Picosecond Pulse Labs (PSPL) Model 4015C pulser (\$11,350) and either the (no longer available) Tektronix 11801B DSO with an SD-24 sampling head or the Tektronix TDS 8000 DSO (\$19,500), with an 80E04 sampling head (\$12,800). This brings the cost of the electronics package to \$43,650. Thus, the electronics cost for a time domain range is about one fourth that for a comparable frequency domain range. Note that there is no problem with dispersive loss in long cable lines, since no fast-risetime signal is carried by cable between transmit and receive electronics.

The second major cost of an antenna measurement system is the anechoic chamber or the real estate required for making the measurements. The propagation path of a time domain range can be relatively close to the ground or other surroundings, perhaps as little as three meters distant. This is possible because reflections from the ground or other surroundings can be easily time-gated out of the main signal. On the other hand, a frequency domain system requires either an anechoic chamber or an outdoor range with the antennas far removed from the ground. These restrictions are necessary in order to reduce or eliminate reflections from walls, floor, or ground.

It is somewhat difficult to assign a cost to the anechoic chamber, or to the real estate required for an outdoor antenna range operating in the frequency domain. Just the absorbing materials for an anechoic chamber can easily cost as much as \$100,000. The cost of a large shielded chamber is additional. Outdoor ranges can be less expensive, if a suitable site can be found spanning a small valley. On the other hand, a time domain system can be set up outdoors, in a relatively small space, with the antennas just three meters above the ground. This clearly results in significant cost savings, but those savings are hard to quantify.

#### **1.4.2. Temperature Stability of Electronics**

The second advantage of a time domain range lies in its immunity to temperature fluctuations. Typically, with VNA measurements, the ambient temperature may change by no more than one Celsius degree between calibration and measurement. No such requirement for temperature stability exists for a DSO. This means that a time domain range can easily be operated within manufacturers' specifications, without recourse to environmental controls.

#### **1.4.3. Convenience and Deployability**

Since the time domain range can be set up quickly and easily in a modest open space, no anechoic chamber and no dedicated real estate are required. This makes it possible to set up the antenna range, align it, calibrate it, collect data, tear it down, and store it away, all within a day.

### **2. Incorporation of Azimuth and Elevation Positioners into the Antenna Range**

Prior to this effort, our time domain antenna range was similar to that depicted in Figure 2, but without the computer controller, and with a manually adjusted tripod head as a positioner. Now, we have added azimuth and elevation positioners with a computer interface. As computer controller, we selected a laptop PC with a GPIB interface to the oscilloscope and a

RS232 serial link to the positioner controller. To permit use of our antennas, with their existing tripod mount hardware, we built an antenna mount to attach our antennas to the positioner hardware.

## **2.1 Positioner Hardware**

For our azimuth and elevation positioners, we selected the Yaesu G-5500 AZ–EL pair. This model features more than 360° of azimuthal travel and a 180° elevation sweep. Although it has less precision (about  $\pm 1$  degree) than we may ultimately want, it is inexpensive, light in weight, and adequate for use with our prototype range. It has the same functionality as heavy, more precise units, at a fraction of their cost. The package includes an analog servo controller and an analog-to-digital computer interface, which connects to a serial port of the range control laptop computer.

## **2.2 Design of the Antenna Mount Interface**

We designed and built a mounting bracket to attach the antenna under test to the positioner. The bracket accepts our standard quick-release (photographic-style tripod head) antenna mount. It also includes counterpoise arms to offset the weight of our heaviest antennas during elevation sweeps.

## **2.3 Configuration of Positioners and Antenna Mount**

The assembled positioner and antenna mount assembly, with no antenna mounted, is shown in Figure 5. Figure 6 shows an assembly drawing of the bracket. The elevation unit is mounted directly to the top of the azimuth unit. The antenna mounting bracket and counterpoise arms form a split ring that cinches the assembly to the horizontal elevation boom. The quick-release antenna (tripod) mount is located at the top center of the mounting bracket. A pair of eight-meter cables permit the positioner controller and computer interface units to be located a convenient distance from the positioners.

An adapter plate allows the elevation positioner to be mounted upside-down on the azimuth unit. This keeps the off-center horizontal axis of rotation of the elevation unit as near the center of the antenna as possible. At an elevation of zero degrees, the axis of rotation of the azimuth unit passes through the center of the quick release mount. This places the center of our

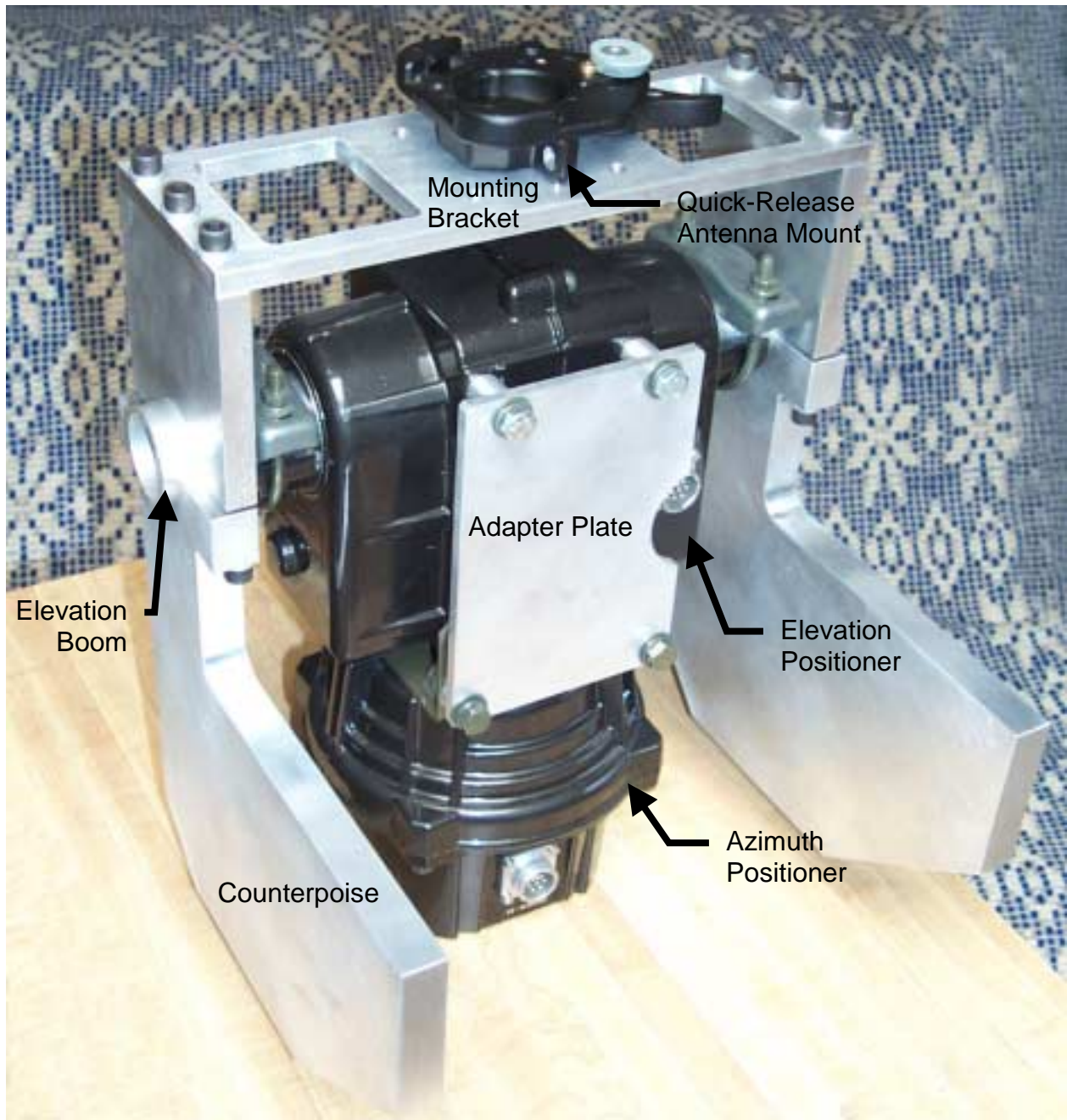


Figure 5. AZ-EL positioners with antenna mounting bracket and counterpoise.

antennas ~15 cm off the vertical axis. Although we could have offset the mount from the axis to compensate, this would have come at the expense of more restricted elevation travel. As it is, the maximum elevation is limited to somewhat under  $90^\circ$  by contact of the mounting bracket with the elevation signal cable. The minimum elevation is about  $-30^\circ$  for our 18-inch IRA.

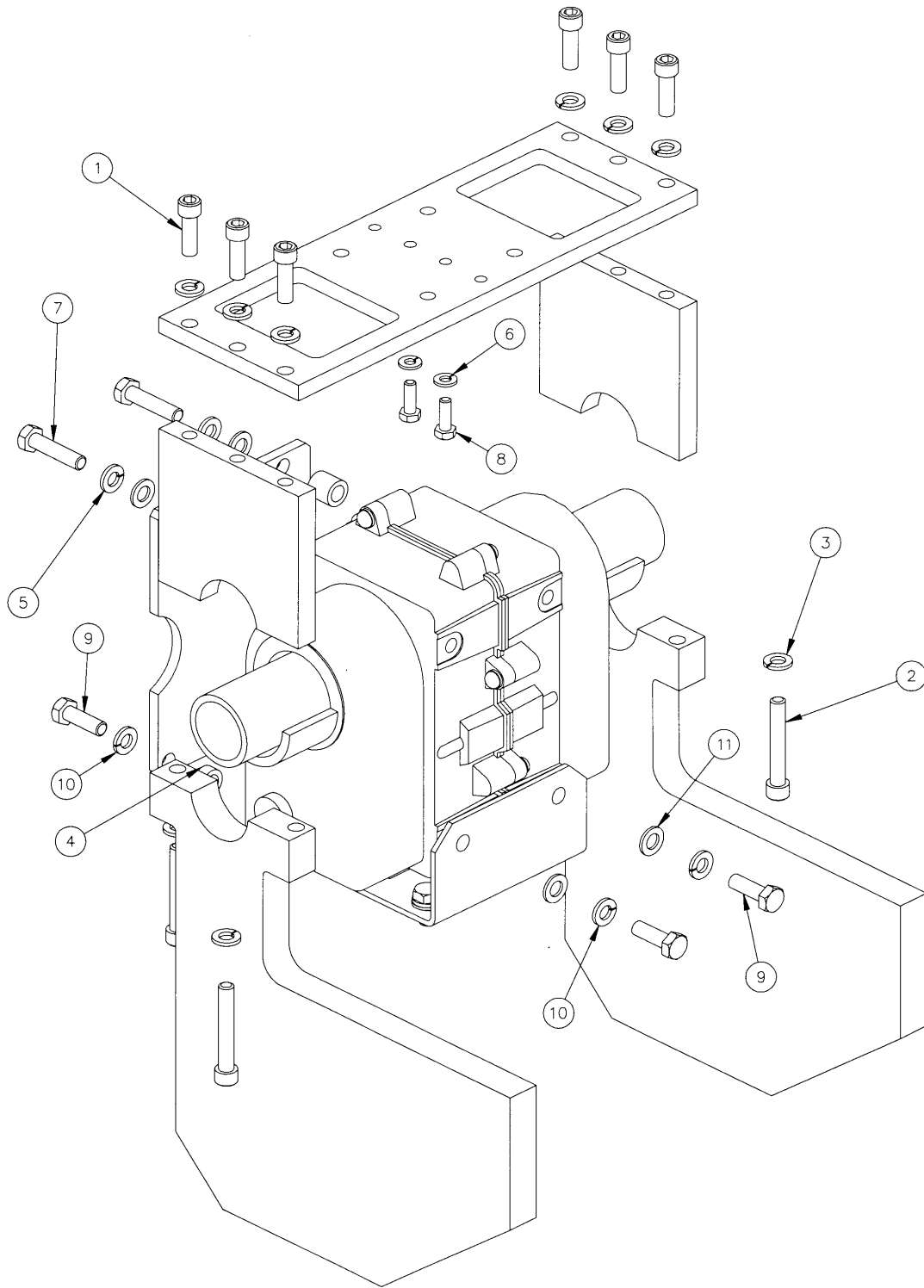


Figure 6. Assembly drawing for antenna mounting bracket and counterpoise with elevation positioner. In use, the bracket at the base of the elevation positioner is bolted to the top of the azimuth positioner.

### **3. Design of the Range Control Software**

We have developed an initial version of time domain range control software, using the National Instruments LabVIEW™ programming environment. This software controls the antenna positioners and data acquisition by the DSO. It also downloads waveform data from the DSO and stores it on the hard disk of the computer controller. This permits automation of the complete sequence of antenna measurements required to characterize antenna response as a function of orientation. Finally, by exploiting LabVIEW's ability to invoke MATLAB® scripts, the range control software can execute routines from our signal processing library, and return the processed data for display in a LabVIEW window. Since the processing required to obtain antenna gain from a single waveform takes only a few seconds, the processed information can be obtained in the midst of the data acquisition protocol and in near-real time.

The range software has been designed within a modular architecture of LabVIEW *virtual instruments* (VIs). Functionally, there are four main modules which are integrated and controlled by the top-level VI, the Range Control Executive, which also provides the primary operator interface to the system. The main modules are: (1) the Antenna Positioner Driver, (2) the Data Acquisition Controller, (3) the Waveform Download and Storage Server, and (4) the Waveform Signal Processing Server. Each of these modules calls upon the services of one or more sub-VIs to accomplish its work. A diagram of the VI hierarchy is shown in the screen image presented in Figure 7. Associations of the VIs shown in the hierarchy with the functional elements of the software are indicated in the following descriptions of those elements.

#### **3.1 Range Control Executive**

The graphical user interface (GUI) of the executive (see the image of the VI panel in Figure 8) supports operator specification of antenna orientations to be sampled at each azimuth within each elevation plane, DSO acquisition parameters, and hard disk locations for storage of acquired waveform data. Signal processing parameters are specified and results displayed by a sub-VI pop-up panel. The software initialization routine (a part of the executive module) provides for manual alignment of the AUT to an operator-determined boresight direction. Once the operator indicates satisfaction with the boresight orientation, the software completes the acquisition and storage of antenna response data for all specified orientations. Next, we describe the operation of the executive in somewhat greater detail.

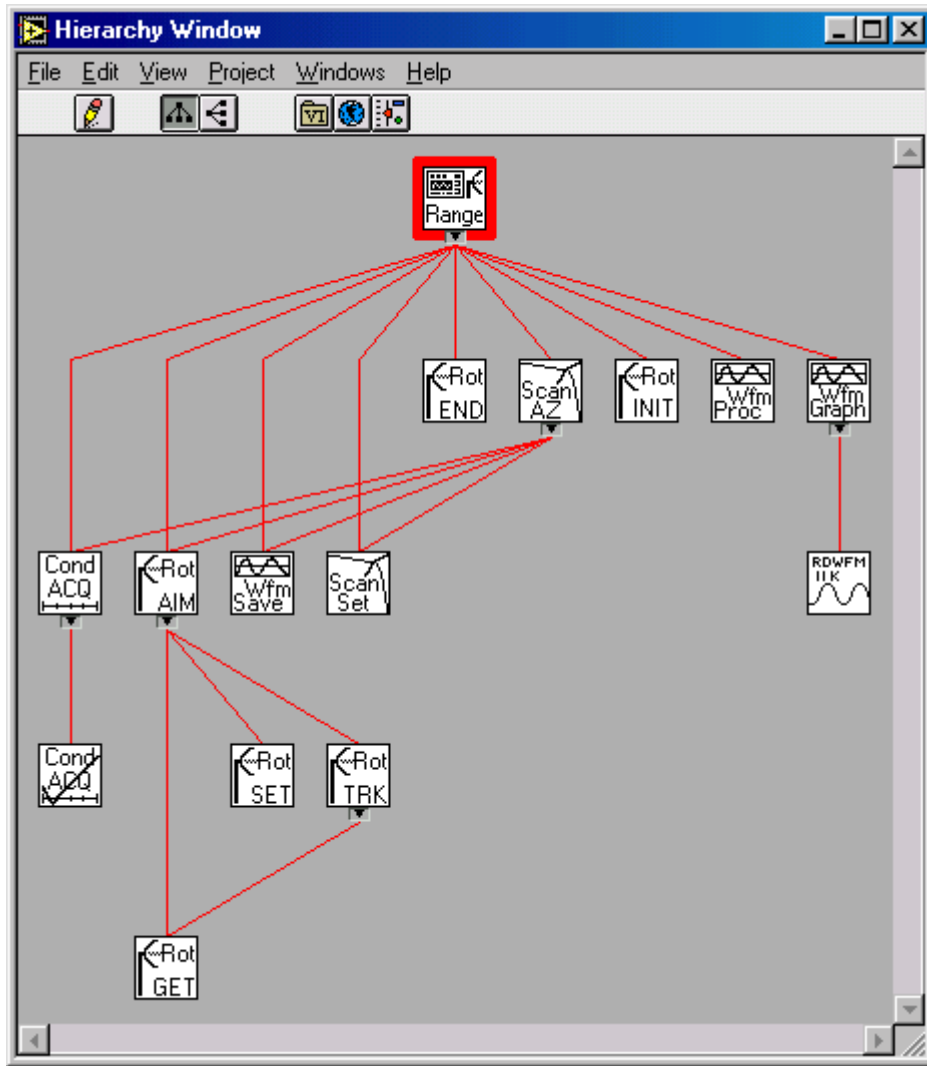


Figure 7. Virtual instrument hierarchy of the range control software.

In response to the user’s “Run” command, the executive initializes the antenna positioner (serial port) and DSO (GPIB) communications channels, by invoking *RotINIT* and several GPIB routines, respectively. Then, it begins and displays a continuous waveform acquisition, while waiting for the user to request, by “Desired Orientation” entries, that the antenna be oriented to boresight. During this time, scan control parameters, the number of traces to be averaged for each waveform, and file storage locations can be adjusted as may be desired. When the user is satisfied with the boresight setting and other entries, toggling the “Set Boresight” switch to “DISABLED” initiates an automated sequence of orientation scanning, waveform acquisition, waveform download and storage, and waveform signal processing. The executive utility sub-VI, *ScanSet*, converts scan limits and step sizes to loop control parameters. *ScanAZ* uses those parameters to execute a sequence of three calls for each required orientation. For each

orientation, *ScanAZ* calls *RotAIM* to reorient the antenna, *CondACQ* to have the DSO acquire a new waveform, and *WfmSave* to write the data to a disk file. At the end of the sequence, the executive invokes *RotEND* to release the serial port, then self-terminates, leaving on disk, a log file containing orientations and saved waveform data file names.

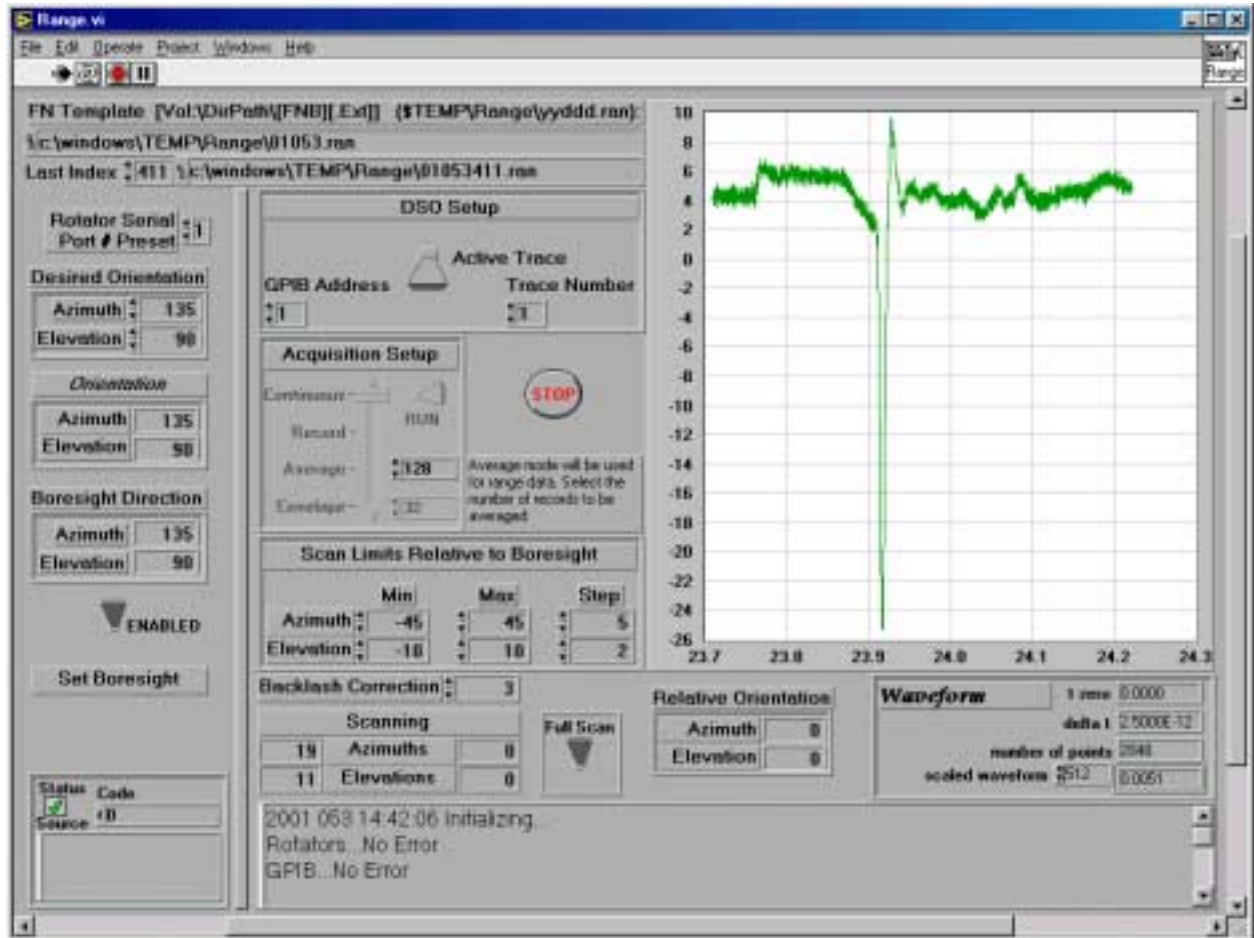


Figure 8. Graphical user interface for the range control software.

### 3.2 Antenna Positioner Driver

Six sub-VIs comprise the antenna positioner driver. They are *RotINIT*, *RotGET*, *RotSET*, *RotTRK*, *RotAIM*, and *RotEND*. These routines all use the LabVIEW *VISA* instrument interface to communicate with the controller for the positioners. Use of these *VISA* routines effectively isolates all positioner communication in platform-independent code. Additionally, only the first three of these routines contain coding specific to the positioner hardware. Only the embedded command and response strings should need to be changed to accommodate a different pair of positioners.

The basic purpose of each of the positioner driver sub-VIs follows:

<i>RotINIT</i>	Connects to the serial port for the positioner controller.
<i>RotGET</i>	Queries the positioner controller to obtain the current orientation.
<i>RotSET</i>	Commands the positioner to adjust to a new orientation.
<i>RotTRK</i>	Monitors and updates the current orientation while the positioner adjusts to a new orientation.
<i>RotAIM</i>	Oversees the process of pointing the positioners to a newly requested orientation, while correcting for system backlash.
<i>RotEND</i>	Terminates communication with the positioner controller and releases the associated serial port.

During initialization, *RotAIM* is invoked by the executive to aim the antenna in response to the user's specification of the desired boresight orientation. During the automated scan, *RotAIM* is invoked by *ScanAZ* to adjust the positioners to each orientation stop.

### 3.3 Data Acquisition Controller

DSO data acquisition is controlled by the *CondACQ* VI. The sub-VI, *CCondACQ*, responds to DSO requests for service, checking for completion of the requested acquisition. These VIs contain DSO-specific command and response strings and programming.

During initialization, *CondACQ* puts the DSO in a continuous acquisition mode, so that the active trace can be monitored while the antenna is being aligned to the boresight direction. During the automated scan, *CondACQ* is invoked by *ScanAZ* to acquire a waveform, consisting of an average of the selected number of consecutive traces, at each orientation stop.

At present, the GPIB bus address of the DSO and the number of data traces to be averaged for each waveform are the only DSO and acquisition setup parameters programmed in the range control software. All other DSO setup must be done on the oscilloscope itself.

### 3.4 Waveform Download and Storage Server

*WfmSave*, *WfmGraph*, and *RDWFM* comprise the download and storage VIs. *RDWFM* performs the actual DSO access to download the current waveform. It is the only one of these VIs containing DSO-specific programming. *WfmGraph* invokes *RDWFM* in a continuous loop, displays the waveform on the computer screen, and updates a global variable with copy of the

waveform. Upon completion of the acquisition for each orientation step, the global variable is read by *WfmSave*, which writes the waveform data to a disk file and makes an entry of the orientation and disk file name in a session log file.

During initialization, *WfmGraph* is started in order to maintain and display a local copy of the latest waveform data. It continues to execute in parallel with all other range control operations. During the automated scan, *WfmGraph* is synchronized with each orientation step, to avoid conflict with acquisition and to ensure that the current waveform is available to *WfmSave*.

### **3.5 Waveform Signal Processing Server**

By use of the Active-X interface between LabVIEW and the MATLAB run time engine, the *WfmProc* VI executes a modification of our MATLAB antenna analysis script to process waveform data and return results to LabVIEW.

In this version of the range control software, *WfmProc* is invoked only once, at the end of initialization, to analyze the boresight waveform. When the boresight waveform has been saved to disk, the *WfmProc* panel pops up (Figure 9). On this panel, the user can specify the default location for normalization data files, the names of source and sensor normalization data files, and filter parameters to be used in deconvolving source, transmit antenna (sensor), and other system contributions from the observed antenna response. Processing can be repeated any number of times with different filtering parameters and/or normalization data. A drop-down menu above the graphical waveform display permits selection of raw data or any of several derived results for viewing. In the current implementation, data acquisition is suspended during processing; and the user must dismiss the processing panel by clicking on the “Resume Acquisition” button to continue. This behavior will ultimately be changed to permit concurrent processing and acquisition of successive waveforms at each orientation step.

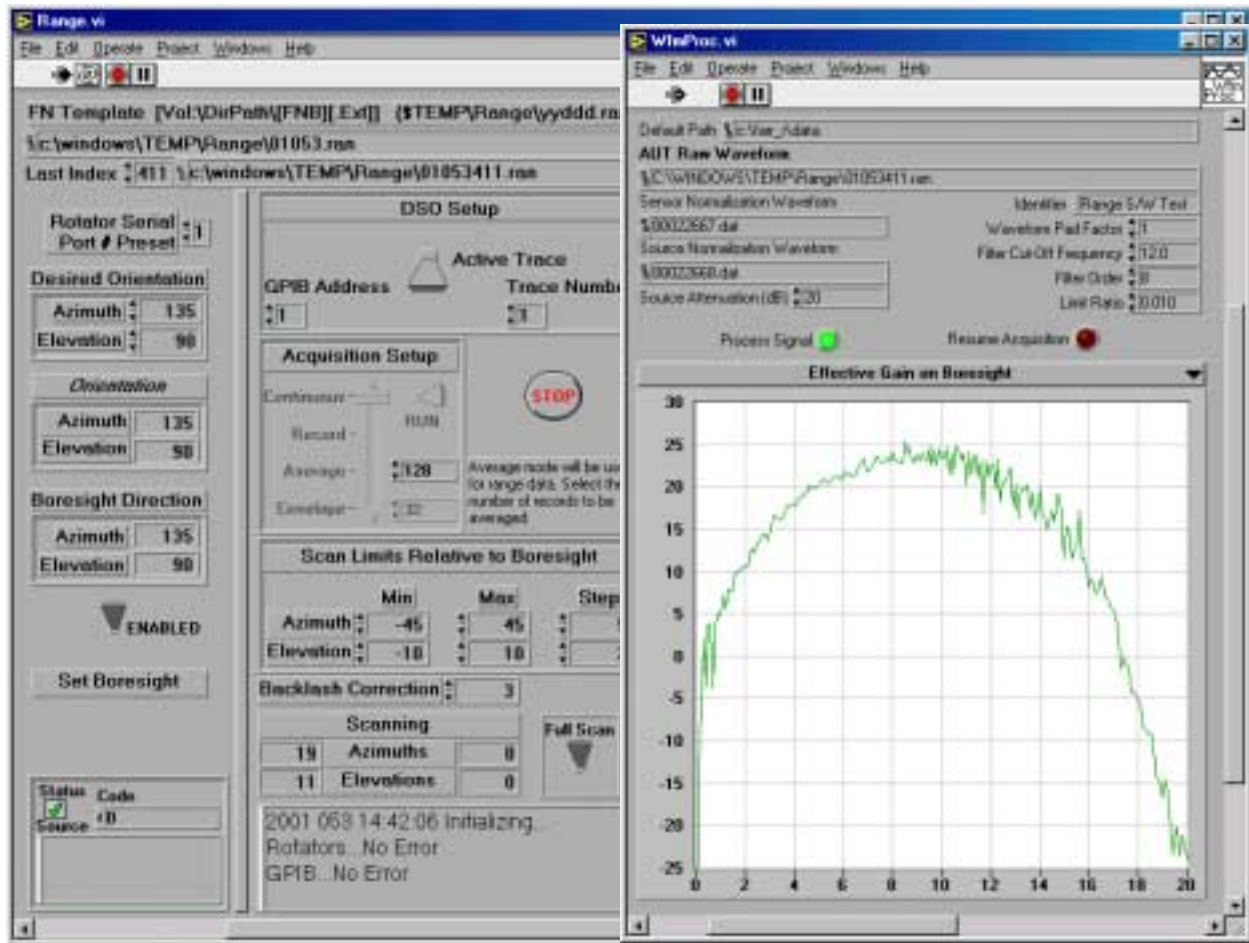


Figure 9. Waveform signal processing popup control and display panel. The popup is invoked by the range control executive to offer the user the option of analyzing the boresight waveform. When the popup is dismissed, the executive resumes the automated measurement sequence.

#### 4. Range Automation Integration

The AZ-EL positioner assembly and a laptop computer with the LabVIEW range control software were installed and tested at our outdoor time domain antenna range. Figure 10 and Figure 11 show photos of the setup. The software was used to orient an 18-inch IRA, while commanding the DSO to acquire waveform data and download it to the laptop for storage. The range control software operated the antenna positioners through a serial port and controlled DSO waveform acquisition and download through a GPIB port. Responding automatically to antenna orientation reports and request-for-service interrupts by the DSO, the software orchestrated the acquisition and storage of antenna response waveform data for desired orientations in **E** and **H** planes. Both Tektronix 11801B and TDS 8000 DSOs have been tested, and the system is now in routine use on our range. Planned and in-progress refinements are discussed later.



Figure 10. Antenna under test at time domain range. The antenna and AZ-EL positioner assembly is mounted on a raised platform affixed to the front wall of the instrumentation shed.



Figure 11. Automated range instrumentation. Positioner controllers and computer running the range control software sit upon a Tektronix 11801B digital sampling oscilloscope.

## 5. Use of a Risetime Filter

Use of a gaussian risetime filter reduces the peak field received at the AUT, permitting the digitizer gain to be turned up. We expected this to provide an improved signal-to-noise ratio (SNR) at low frequencies, at the expense of high-end bandwidth. We selected a 70 ps filter to slow the risetime of the output step of the PSPL 4015C pulser from  $\sim 30$  ps to  $\sim 75$  ps, as indicated in Figure 12.

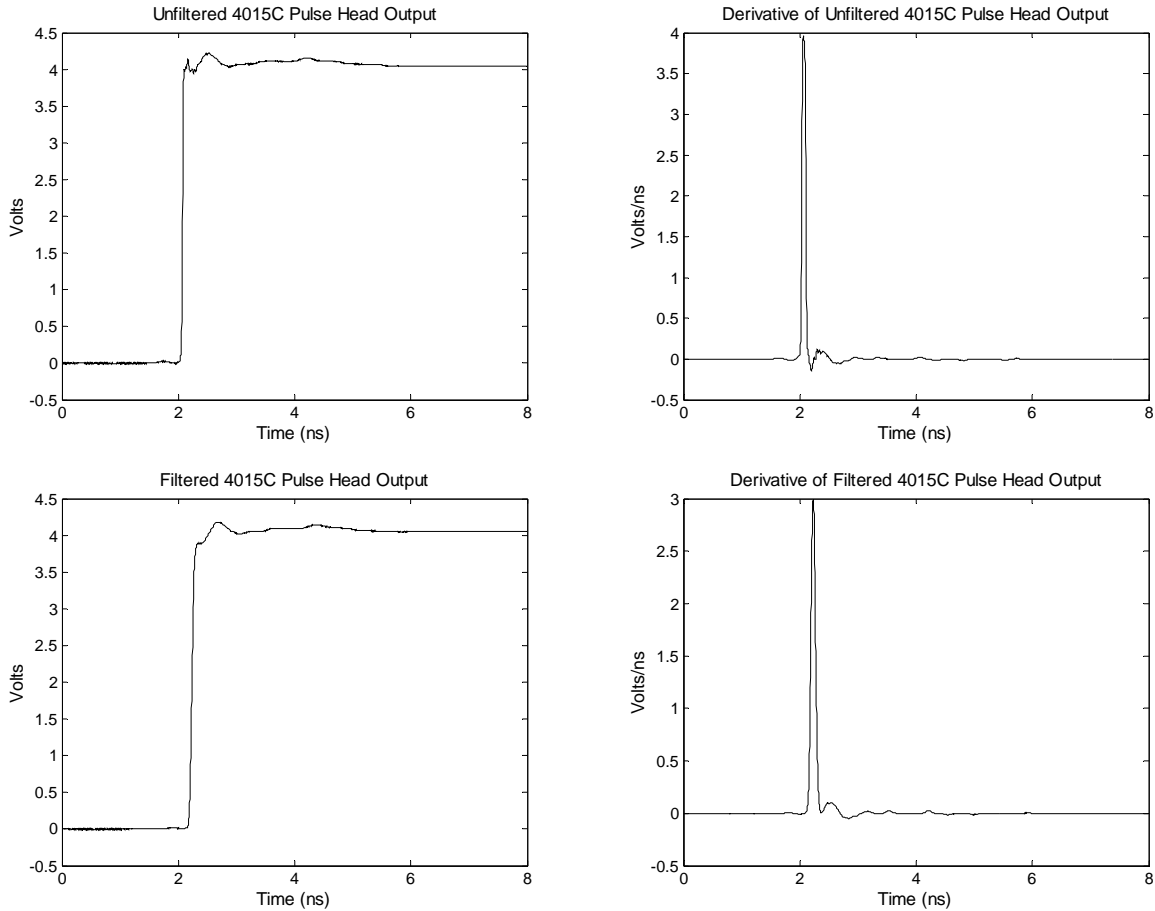


Figure 12. Unfiltered and filtered PSPL 4015C output voltage steps and their derivatives.

The effective gain of an IRA-2 antenna was measured without and with the risetime filter (Figure 13). The raw peak response was reduced about one third by the filter. This reduction does not allow a meaningful increase in the digitizer gain. A slower filter, perhaps on the order of 150 ps, might permit a significant increase in digitizer gain. The effective gain calculations agree well up to about 8 GHz, where they peak at 24.5 dBi. Beyond that, the filtered data becomes unusable because of the 10 GHz low-pass filter used in the signal processing (Figure 14 and Figure 15).

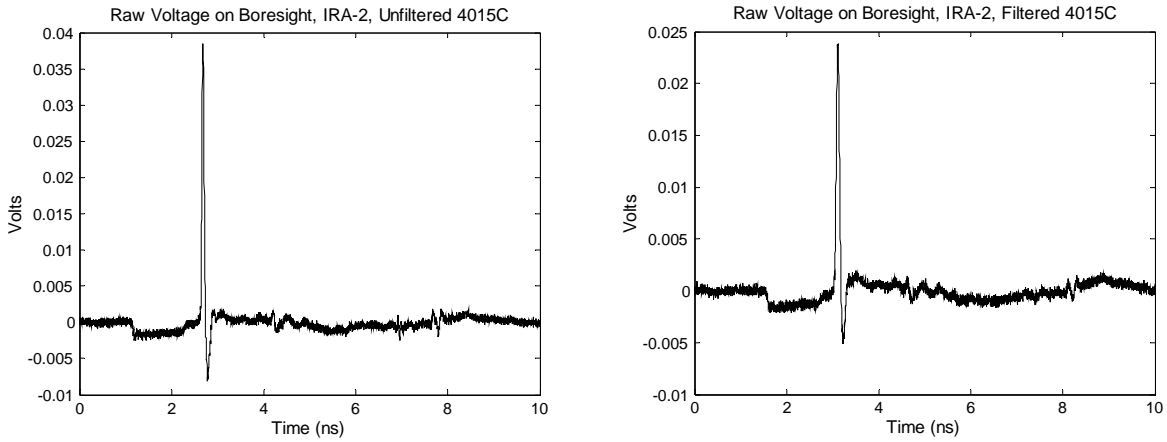


Figure 13. Raw response of the IRA-2 for unfiltered and risetime-filtered PSPL 4015C. The unfiltered peak response is 38 mv, with a FWHM of 51 ps. With the 70 ps gaussian risetime filter, the peak response is 24 mv, with a FWHM of 75 ps.

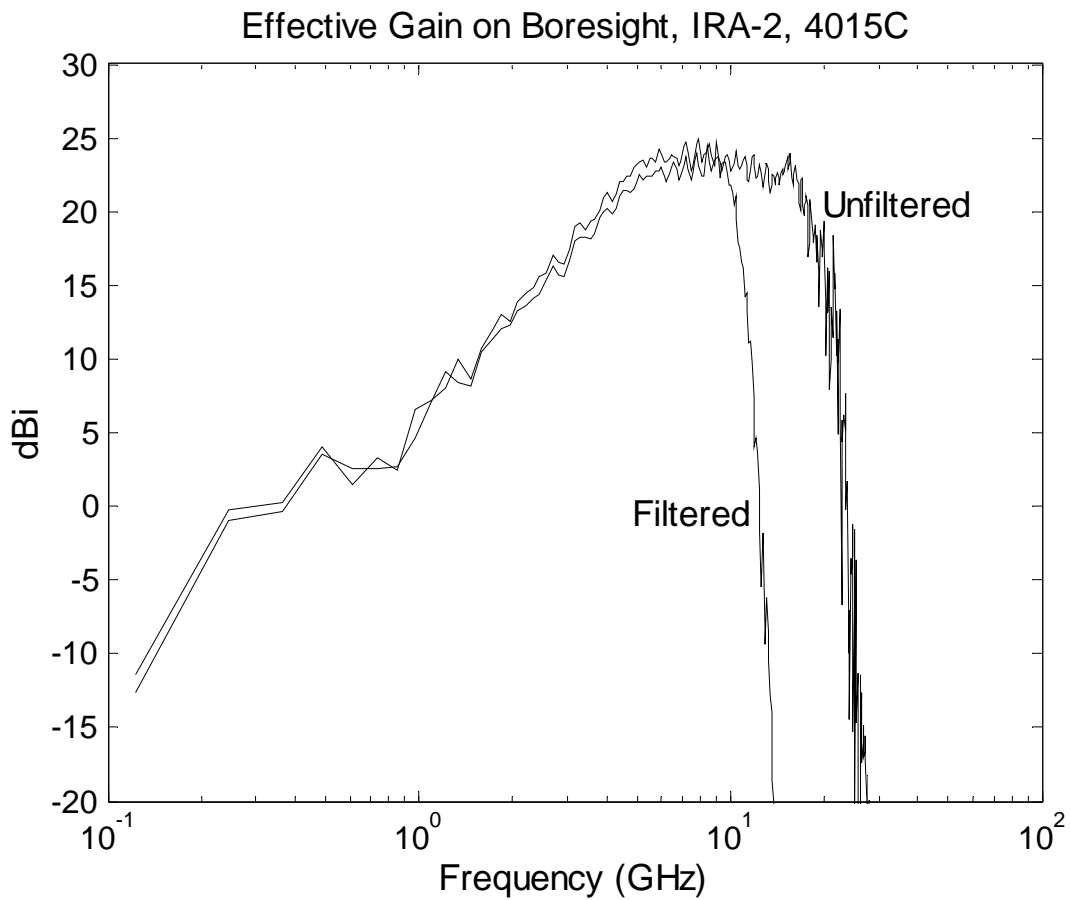


Figure 14. IRA-2 gain comparison, risetime-filtered and unfiltered source (semi-log plot).

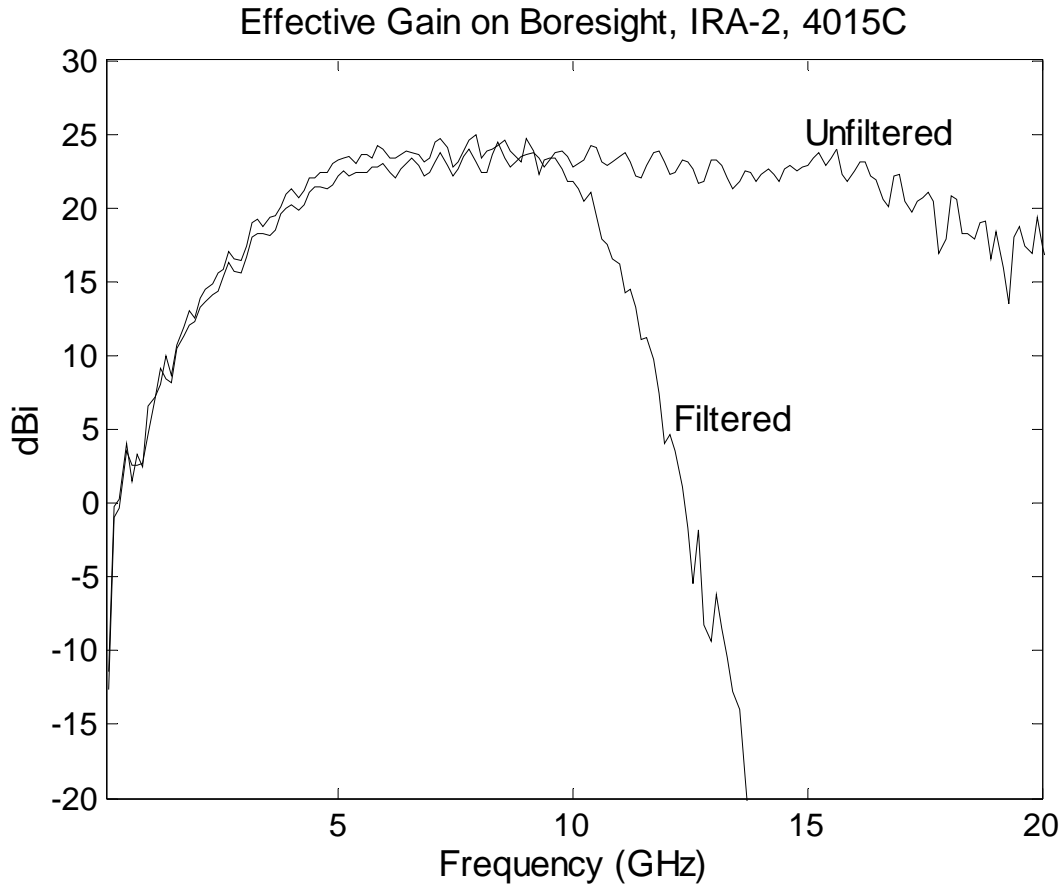


Figure 15. IRA-2 gain comparison, risetime-filtered and unfiltered source (linear plot).

## 6. Mitigation of Ground Bounce

We examined the use of a simple hardware-cloth reflector as a ground bounce diverter. Normally, ground bounce would be time-gated out during signal processing. However, if the response is broad, either because of a slow source or as a result of risetime filtering, it may not be practical to gate out the ground bounce. We found that a tent-shaped reflector, on the ground, with ridge line along the boresight direction, could eliminate nearly all traces of ground bounce. This is reminiscent of an approach used with horizontally polarized, guided-wave EMP simulators to reduce the contribution of reflected energy to the test volume [3]. The effectiveness of the reflector is demonstrated by Figure 16. The erected reflector is shown in Figure 17. The reflector was recently lengthened to improve its coverage for low antenna look angles, and mounted on a PVC frame to make setup easier.

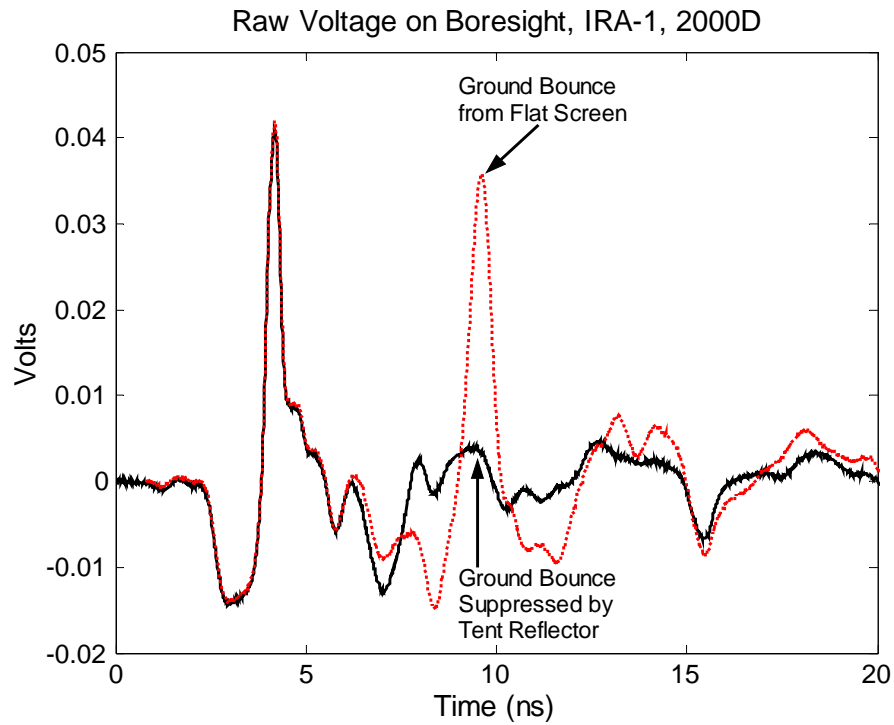


Figure 16. Mitigation of ground bounce by a tent-shaped metal mesh reflector.



Figure 17. Tent-shaped reflector for mitigation of ground bounce. The ridge line of the metal mesh is parallel to the boresight direction.

## 7. Planned Range Design Refinements

The automated time domain range, as described above, is a prototype, featuring somewhat coarse antenna orientation control and limited signal processing capabilities. Design refinements in hardware and software will lead to a fully integrated and automated system with the necessary antenna pointing precision and a full set of the best available online signal processing functions. Reaching this goal will require research bearing on key implementation issues, and will culminate in production of a complete turnkey system.

### 7.1 AZ-EL Positioners and Mounting Hardware

When we selected the Yaesu G-5500 positioners for the prototype range, we realized that their precision ( $\pm 1$  degree) might not be adequate for a production range. Another consideration bearing on positioner design is the potential for interference of the positioner with the antenna measurement. While this is not a major concern with dish antennas like the IRA, which do not radiate strongly in the backward direction, for most other antenna designs, a bulky metallic positioner co-located with the antenna would be a significant source of interference. A third issue arises from the goal of flexible deployment of the time domain range. On level terrain, such as we have at our present range site, it is easy to align the elevation-over-azimuth Yaesu positioners to scan **E** and **H** planes. One sets the elevation and azimuth axes normal to the boresight direction. On sloping terrain, the boresight elevation becomes non-zero. Unless the antenna mast is tipped to remain normal to boresight, the positioners will not trace **E** and **H** plane paths.

After reviewing commercially available positioner/mast assemblies, we concluded that we could best address the three issues identified above by designing our own positioner/mast hardware. The following sketch (Figure 18) represents our preliminary design approach. To minimize metallic parts near the antenna, positioner motors are mounted at the base of a non-metallic mast. A pair of toothed belts drives the azimuth platform and elevation boom at the top of the mast. The only metal parts at the top are some gears and the antenna mount. Positioning accuracy is addressed by use of precision stepper motors with appropriate reduction gearing. We expect to achieve a precision of  $\pm 0.1$  degree. The sloping terrain issue is addressed by mounting both azimuth platform and elevation boom at the top of the mast and in an azimuth-over-elevation configuration. With this approach, the mast remains vertical. We compensate for sloping terrain by an adjustment of the elevation positioner. Residual **E** and **H** plane path errors may be compensated in software.

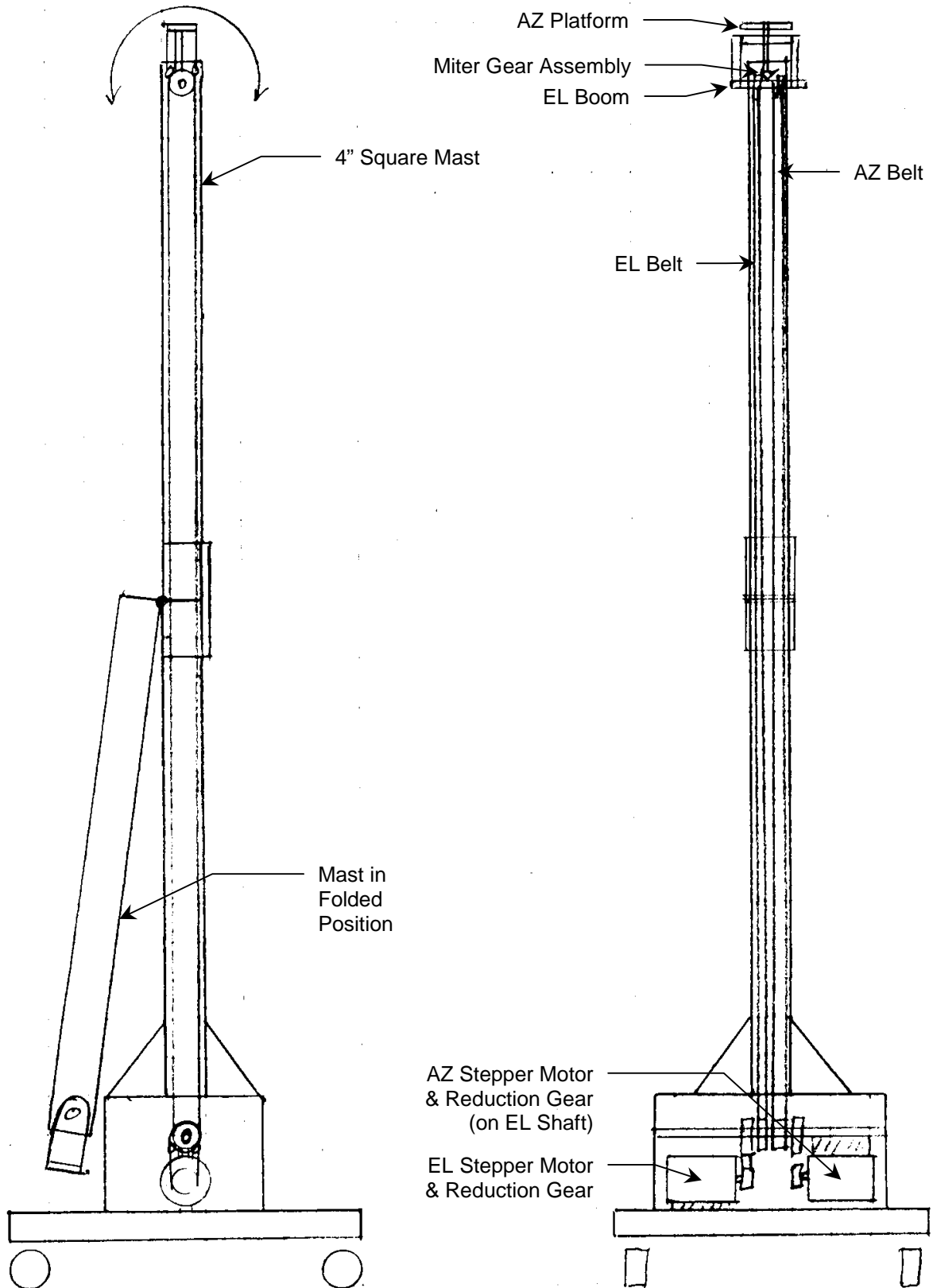


Figure 18. Azimuth-over-elevation antenna positioner and mast assembly with belt-driven azimuth platform and elevation boom.

## 7.2 Deconvolution Algorithm

There are two facets to the challenge of automating signal processing for the time domain range. The easier of these to solve has already been accomplished—incorporation of signal processing within the range control software. The more difficult issue is automation of the signal processing algorithms, themselves—eliminating the need for user tweaking of processing control parameters on a case-by-case basis. As a foundation for achieving reliable automated processing, we plan to research the mathematics issues relevant to deconvolution and low-pass filtering. Based on this research, we will select the most robust approach, consistent with processing automation.

Without low-pass filtering, deconvolution of the system response from the measured response to obtain the response of the AUT can easily become dominated by numerical noise, since neither the system response nor the measured response is precisely known. Our existing routines employ a “modified” (non-causal) Butterworth filter. This filter is specified by three parameters, the 3 dB cutoff frequency, the filter order, and a limit ratio. The latter is similar to a frequency-independent minimum SNR; it keeps the deconvolution from “blowing up.” It is a loose interpretation of Riad’s implementation [4] of Nahman’s optimal deconvolution [5]. In current practice, the three parameters are adjusted recursively until the response “looks right.” While reasonably effective, this approach can be tedious; and it is not amenable to automation. Moreover, the use of a non-causal filter leads to the appearance of Gibbs’ phenomenon in the form of a ringing signal *before* the arrival of the deconvolved impulse.

We plan to investigate three potential alternatives to our current approach: 1) use of a causal low pass filter, e.g., a “true” Butterworth, 2) application of a strict interpretation of Nahman’s optimal deconvolution, and 3) use of a total least squares (TLS) fit, which determines the pseudo-inverse of the antenna response with a singular-value decomposition, as described by Rahman and Sarkar [6]. The latter is related to the matrix pencil method, and has been used successfully in a time domain RCS application by a group from The Netherlands [7]. As the Butterworth is no more amenable to automation than our current approach, we expect to concentrate our research on Nahman’s optimal deconvolution and Sarkar’s TLS approach. At present the TLS approach appears most promising, as it can be completely automated, with no requirement for tweaking of parameters.

### 7.3 Automation

While the new deconvolution algorithm will reduce the need for user intervention in the analysis process, we also contemplate a more thorough automation of the entire antenna measurement scenario. Operations which are ancillary to orientation scanning, measurement, and analysis could be brought under the umbrella of the range control software package. This might include complete DSO setups, source normalization measurement, transmitting antenna (sensor) calibration, and TDR measurements of the AUT. The TDR data will be *required*, if we are to provide standard IEEE gain as an output of the signal processing algorithms. Currently, we provide only effective gain, which is the IEEE gain reduced by return loss.

### 7.4 Packaging

Finally, based on chosen antenna positioners, controller(s), alignment tools, pulser, transmit antenna (sensor), DSO, and computer, we will design packaging to support transportation and easy setup, use, and tear-down of the complete automated time domain antenna range system. We expect that a complete system will include the following items:

- (a) Laptop computer with AZ-EL (serial) and DSO (GPIB) interfaces
- (b) Range control and processing software
- (c) AZ-EL antenna positioner and mast assembly
- (d) AZ-EL controller(s)/computer interface
- (e) Tektronix TDS-8000 DSO with 80E04 sampling head and extender
- (f) Farr Research Calibrated TEM Sensor, Model FRI-TEM-01-50 (to be used as the transmitting antenna)
- (g) Picosecond Pulse Labs 4-volt rep-rated pulse generator, Model 4015C
- (h) Antenna alignment tools
- (i) Materials for ground-bounce mitigation
- (j) Mounting fixtures and packaging for use, storage, and transport.

## 8. Concluding Remarks

In the effort described here, we assembled a prototype automated antenna measurement system. The system features full computer control both of the orientation (azimuth and elevation) of the antenna under test, and of sequenced data acquisition by a digital sampling oscilloscope. User-assisted processing of boresight response data to obtain effective antenna gain is also included.

In current and future work, we will refine the physical package to make it compact, rugged, and easy to set up, stow, and transport. We will also enhance the software to provide full system automation, including data acquisition sequencing and complete signal processing, to provide online, near-real-time recovery of complete antenna response data in both time and frequency domains. We will automatically deconvolve the system response from the measured response. Our goal is a turnkey, fully field-deployable system, covering a broad frequency range. We expect the accuracy of the new time domain automated antenna range to be comparable to that of conventional frequency domain ranges.

## References

1. L. H. Bowen, E. G. Farr, and W. D. Prather, "Fabrication and Testing of Two Collapsible Impulse Radiating Antennas," *Sensor and Simulation Note 440*, Dec. 1999.
2. E. G. Farr, L. H. Bowen, G. R. Salo, J. S. Gwynne, C. E. Baum, W. D. Prather, and T. C. Tran, "Studies of an Impulse Radiating Antenna and a Pulse Radiating Antenna Element for Airborne SAR and Target Identification Applications," *Sensor and Simulation Note 442*, Mar. 2000.
3. C. E. Baum, et al., "Electromagnetic Design Calculations for ATLAS I, Design 1," *Sensor and Simulation Note 153*, June 1972.
4. S. M. Riad, "Instructional Opportunities Offered by the Time-Domain Measurement Technology," *Time-Domain Measurements in Electromagnetics*, E. K. Miller, Ed., pp. 72-93, Van Nostrand Reinhold Co., NY, 1986.
5. N. S. Nahman, "Software Correction of Measured Pulse Data," *Fast Electrical and Optical Measurements*, Vol. I, J. E. Thompson and L. H. Luessen, Eds., pp. 351-417, Martinus Nijhoff Publishers, The Netherlands, 1986.
6. J. Rahman and T. K. Sarkar, "Deconvolution and Total Least Squares in Finding the Impulse Response of an Electromagnetic System from Measured Data," *IEEE Transactions on Antennas and Propagation*, Vol. 43, No. 4, pp. 416-421, Apr. 1995.
7. W. A. van Cappellen, R. V. de Jongh, and L. P. Ligthart, "Potentials of Ultra-Short-Pulse Time-Domain Scattering Measurements," *IEEE Antennas and Propagation Magazine*, Vol. 42, No. 4, pp. 35-45, Aug. 2000.